Journal of the European Ceramic Society 17 (1997) 843–850

PII: S0955-2219(96)00136-7
0955-2219/97/$17.00

Preparation of High-Strength (Mg,Y)-Partially Stabilised Zirconia by Hot Isostatic Pressing

F. Meschke,[a] N. Claussen,[a] G. De Portu[b] & J. Rödel[c]*

[a]Technische Universität Hamburg-Harburg, Advanced Ceramics Group, 21073 Hamburg, Germany
[b]National Research Council, Research Institute for Ceramics Technology, 48018 Faenza, Italy
[c]Technische Hochschule Darmstadt, Ceramics Group, 64295 Darmstadt, Germany

(Received 16 April 1996; accepted 23 July 1996)

Abstract

Fine-grained (Mg,Y)-PSZs containing small amounts of spinel as a second phase have been produced by pressureless sintering and hot isostatic pressing. Their mechanical properties have been optimised by judicious adjustment of processing parameters such as sintering temperature, cooling rate and holding time of eutectoid heat treatments. Hot isostatic pressing reduces the internal defect size in comparison with conventional sintering. Without exploiting transformation toughening, high strength values of more than 700 MPa are obtained, which rise to about 900 MPa after eutectoid ageing. Failure mechanisms are discussed in terms of defect size, defect type and R*-curve behaviour.* © *1997 Elsevier Science Limited. All rights reserved.*

1 Introduction

Magnesia-partially-stabilized zirconia (Mg-PSZ) exhibits strong *R*-curve behaviour due to transformation toughening with peak fracture toughness up to 20 MPa $\sqrt{m}$.[1–3] The underlying mechanism is the stress-induced tetragonal (t)–monoclinic (m) phase transformation. The key to get high fracture toughnesses in Mg-PSZ is to maximise the amount of transformable tetragonal phase by eutectoid and/or subeutectoid ageing treatment and optimised cooling rate.[4–6]

The *R*-curve behaviour contributes to respectable strength values in spite of the coarse-grained microstructure consisting of grains with a size of ~50 μm. The large grain size is caused by the high sintering temperatures of more than 1700°C. Strength values up to 700 MPa are characteristic of Mg-PSZ materials of the high strength category.[7,8] Zirconia ceramics with high toughness, however, exhibit generation of surface flaws and a particularly shallow *R*-curve behaviour due to a low critical stress for transformation. Both contribute to strength reduction in spite of enhanced plateau toughness.[7–10]

Refinement of grain size in peak-strength Mg-PSZ should allow for a decrease of effective defect size and higher strengths.[11] Recently, a fine-grained Mg-PSZ type material has been produced by pressureless sintering with the aid of $MgAl_2O_4$ particles.[12–14] Yttria was added as co-stabiliser in order to prevent the phase decomposition occurring in Mg-PSZ between 900°C and 1400°C.[15,16] The benefit of yttria as co-stabiliser has been verified earlier in coarse-grained (Mg,Y)-PSZs.[17,18] Unfortunately, however, overstabilisation results if the MgO content remains unchanged. This leads to a degradation of mechanical properties. In a previous study it has been shown that (Mg,Y)-PSZ materials with a tailored stabiliser content can exhibit a remarkably improved resistance against subeutectoid degradation without any loss of toughness and strength.[14] In the present study the microstructure and the mechanical properties of the pressureless sintered (Mg,Y)-PSZs are evaluated and related to the processing parameters such as sintering temperature, cooling rate and eutectoid ageing time. Furthermore, hot isostatic pressing (HIP) was examined as densification method. In the past, several attempts have been made to age hot isostatically pressed or hot-pressed Mg-PSZ in air. Even after short annealing times, however, severe degradation has been observed by bloating or transformation.[19,20] In this study results are presented on how hot isostatic pressing and ageing in nitrogen atmosphere can significantly enhance the fracture strength of (Mg,Y)-PSZs.

2 Experimental Procedure

As starting materials for the (Mg,Y)-PSZs, commercial powders of stabilised zirconia (Tosoh

*To whom correspondence should be addressed.

TZ3Y and MEL SCMG3·4 grade) were used together with $MgAl_2O_4$ spinel (CERALOX). From the zirconia powders a mixture with a stabiliser content of 0·5 mol% Y_2O_3 and 7·8 mol% MgO was prepared and 3 vol% of $MgAl_2O_4$ was added. The complete powder mixture was attrition milled for 4 h with ethanol in a polyethylene-lined recipient. After liquid sieving and rotovap-drying the powder was crushed and finally passed through a 140-μm grid sieve.

Powder compacts were prepared by uniaxial pressing at 31 MPa with stearic acid as pressing aid followed by cold isostatic pressing at 500 MPa. Sintering in air was performed either at 1720° or 1750°C for 30 min. Cooling rates between 6 and 19 K/min were used. Hot isostatic pressing was performed at 1720°C for 20 min in nitrogen atmosphere at a pressure of 180 MPa. The cooling rate was 19 K/min in this case. Specimens for HIPing were first presintered at 1500°C for 1 h in order to obtain gas-tight samples.

Some specimens were aged at 1400°C for 0–3 h in order to evaluate whether eutectoid heat treatment does improve strength and toughness. The ageing procedure was part of the whole sintering cycle, hence samples were not cooled to room temperature prior to ageing. Referring to the cooling rates the pressureless sintered samples are called S6, S12, S15 and S19 whereas the HIPed samples are named HIP19.

From as-sintered and eutectoidly annealed samples bend bars were prepared by cutting, grinding and polishing. Final dimensions were 3 × 4 × 35 mm^3. A mirror-like surface finish was obtained using 1 μm diamond paste. Toughness was measured on five samples of each material using the single-edge-precracked-beam (SEPB) method.[21,22] A sharp precrack was obtained from three indents of 196 N on the tensile side of the bend bars. The ratio of crack length to specimen height, a/w, was about 0·3. The indents were removed by renotching the cracks with a saw blade of 200 μm width and a sharp pre-crack ahead of the notch of 500 μm length remained. Specimens were subsequently annealed at 900°C for 20 min in order to retransform any m-phase caused by the preparation. Maximum stress of precracked specimens was measured in four-point bending with outer and inner spans of 12 and 6 mm, respectively. Toughness was then calculated according to standard DIN 51109.[23] Bend strength of at least five polished samples was measured by four-point bending according to standard DIN 51110[24] except that outer and inner spans were of dimensions 20 and 10 mm, respectively.

Stress-strain curves were measured using strain gauges in order to determine critical stresses for transformation from the yield stress. The yield stress was defined as that stress where deviation from the linear behaviour by 0·3% occurs. The critical stress for transformation, σ_m^c, was calculated from the yield stress, σ_y, according to Ref. 7:

$$\sigma_m^c = \frac{(1 + \nu)}{3} \sigma_y$$

where a value of 0·31 was chosen for Poisson's ratio, ν.

The tensile sides were examined with optical microscopy after fracture in order to check whether plastic deformation had occurred on the surface. SEM was used in order to characterise the failure origins on fracture surfaces as well as to determine the grain size. X-ray diffractometry with Cu K_α radiation was applied on polished and fracture surfaces in order to determine both phase composition and transformable t-phase volume.

3 Results

3.1 Sintered (Mg,Y)-PSZ

3.1.1 Microstructure

Mean grain sizes of sintered (Mg,Y)-PSZ materials are 13 μm and 19 μm after sintering at 1720°C and 1750°C, respectively. The microstructure of S19, which is characteristic for the pressureless sintered materials, is presented in Fig. 1. A homogeneous distribution of small pores with a size of 1 μm is apparent. Spinel particles appear black and are located at grain boundaries as well as within cubic grains. However, some isolated large pores of diameter up to 160 μm were also observed.

The cooling rate determines the transformable t-phase content and fracture toughness after sintering (Fig. 2). With increasing cooling rate the

Fig 1. Microstructure of 3 vol% $MgAl_2O_4$ spinel containing (Mg,Y)-PSZ after pressureless sintering at 1720°C. Spinel particles appear black.

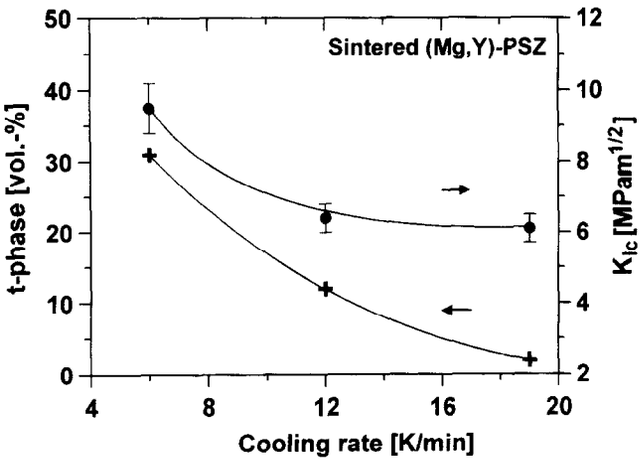

Fig. 2. Transformable t-phase content and fracture toughness in pressureless sintered (Mg,Y)-PSZ as function of cooling rate.

amount of transformable t-phase is reduced from 31 vol% at 6 K/min down to 2 vol% at 19 K/min. Fracture toughness scales with the amount of transformable t-phase and is reduced from 9·5 MPa √m at 6 K/min to 6·1 MPa √m at 19 K/min.

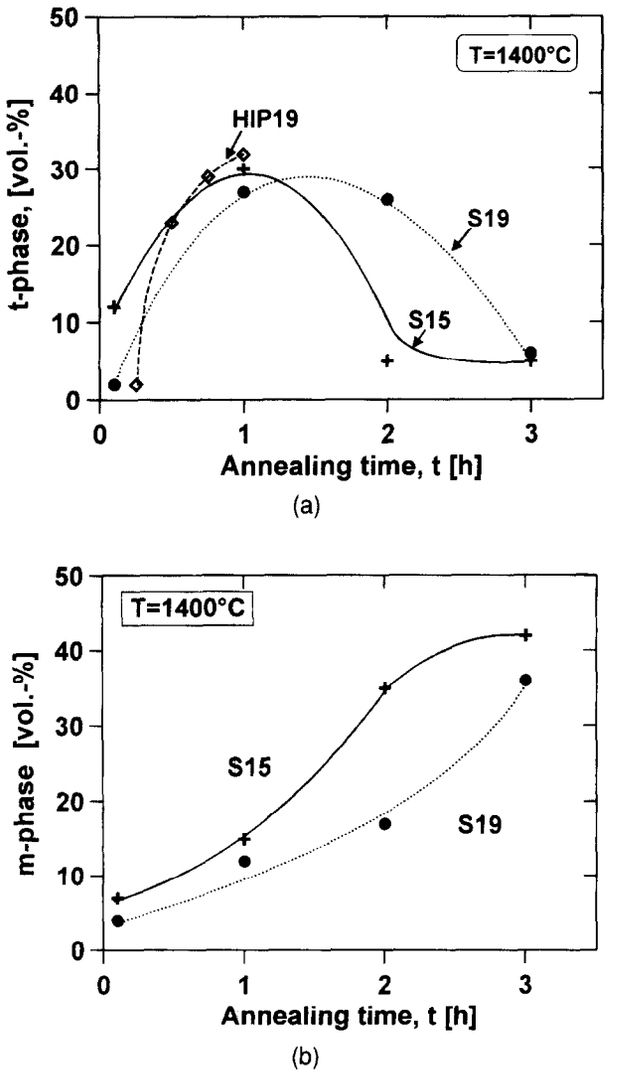

Fig. 3. (a) Transformable t-phase and (b) m-phase content in pressureless sintered and HIPed (Mg,Y)-PSZ after eutectoid ageing at 1400°C.

Fig. 4. TEM micrograph of t-precipitates in peak-aged S19.

The amount of transformable t-phase can be increased in rapidly cooled samples by eutectoid ageing. As shown in Fig. 3(a) for specimens cooled at 15 and 19 K/min, respectively, a t-phase content of about 30 vol% can be obtained in S15 after 1 h. Peak ageing is achieved in S19 after 1·5 h, i.e. at 30 min prolonged ageing time. Over-ageing occurs after 2 h and reduces the transformable t-phase and increases the m-phase content sharply as well. The m-phase content then rises from 4 vol% in the as-sintered S19 specimens to 35 vol% after 3 h of ageing (Fig. 3(b)).

The t-precipitates formed during ageing have a lens-shaped morphology (TEM-micrograph in Fig. 4). Their diameter is about 190 nm in peak-aged samples of S19. Overaged precipitates in the S19 material have a size of 300 nm and are heavily twinned.

3.1.2 Failure origins

The fracture surfaces reveal pores with diameters ranging from 40 to 160 μm. A typical failure origin located close to the tensile side is shown in Fig. 5. A purely transgranular fracture mode is evident from the micrograph.

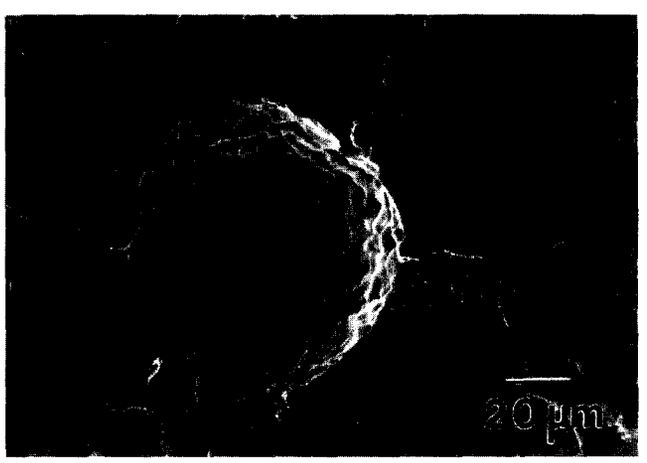

Fig. 5. Fracture surfaces of as-sintered S19 with a spherical pore close to the tensile side.

3.1.3 Stress-strain behaviour

Linear-elastic stress-strain behaviour up to the fracture stress is observed in unaged specimens of S15 and S19. In the aged high-toughness materials, plastic deformation during flexure becomes apparent from the stress-strain curves presented in Figs 6(a) and (b). The yield stresses indicating the onset of the t → m transformation decrease in the S15 specimens with ageing time from 405 MPa after 1 h to 310 MPa after 3 h. The corresponding values for S19 are 515 and 280 MPa, respectively. Table 1 summarises the critical stresses for transformation calculated from the yield stresses.

Plastic deformation due to transformation is evidenced also by surface uplift on the tensile side of bend bars. Fig. 7(a) shows an optical micrograph from which the volume expansion associated with the t → m transformation and microcrack formation is visible.

3.1.4 Mechanical properties

Toughness is increased by ageing treatment from 6·0 MPa √m up to 11·2 MPa √m in S15. Comparison of Figs 8(a) and (b) shows that strength scales with toughness. Strength is improved in S15 from 466 MPa to 692 MPa after 1 h at 1400°C. Similar results are obtained for S19 specimens. Toughness and strength rise up to 10·5 MPa √m and 601 MPa after ageing for 1 and 2 h. An interpolation of the data in Figs 8(a) and (b) shows that peak strength and toughness are achieved for each material at the same ageing time. Peak values are obtained after about 1 and 1·5 h of ageing in S15 and S19, respectively, which correlates with the optimum in transformable t-phase (Fig. 3(a)).

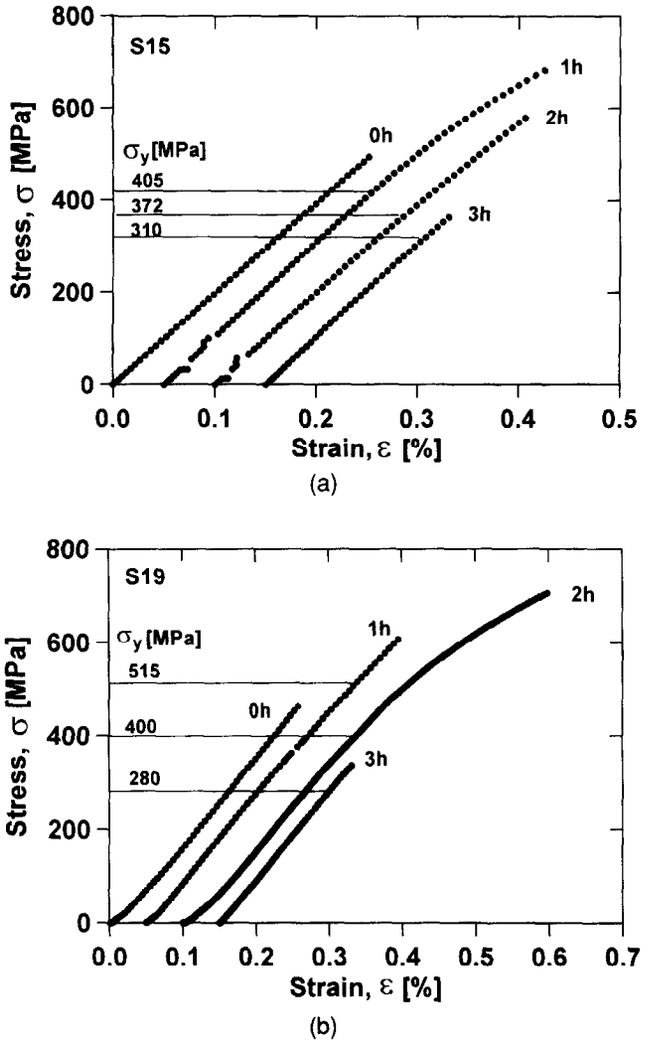

Fig. 6. Stress-strain curves of (a) S15 and (b) S19 after different ageing treatments.

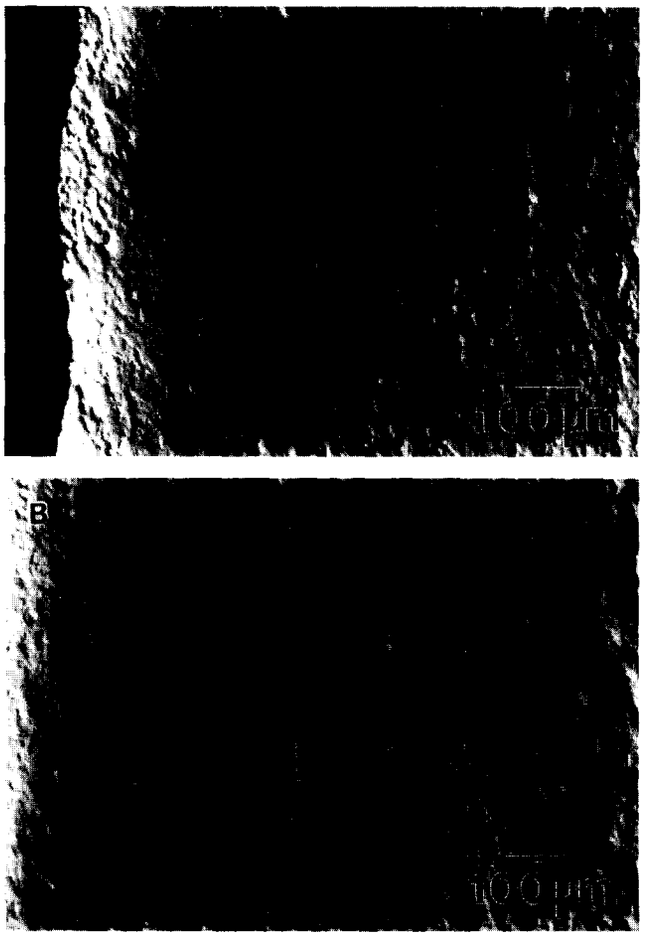

Fig. 7. Plastic deformation on tensile side of peak-aged (a) S15 and (b) HIP19 bend specimens.

Table 1. Yield stresses and critical stresses for transformation in [MPa]

S15	σ_y	σ_m^c	*S19*	σ_y	σ_m^c	*HIP19*	σ_y	σ_m^c
As-fired	>550	240	As-fired	>450	>262	As-fired	>800	349
1 h	405	177	1 h	515	225	30 min	420	183
2 h	372	162	2 h	400	175			
3 h	310	134	3 h	280	122			

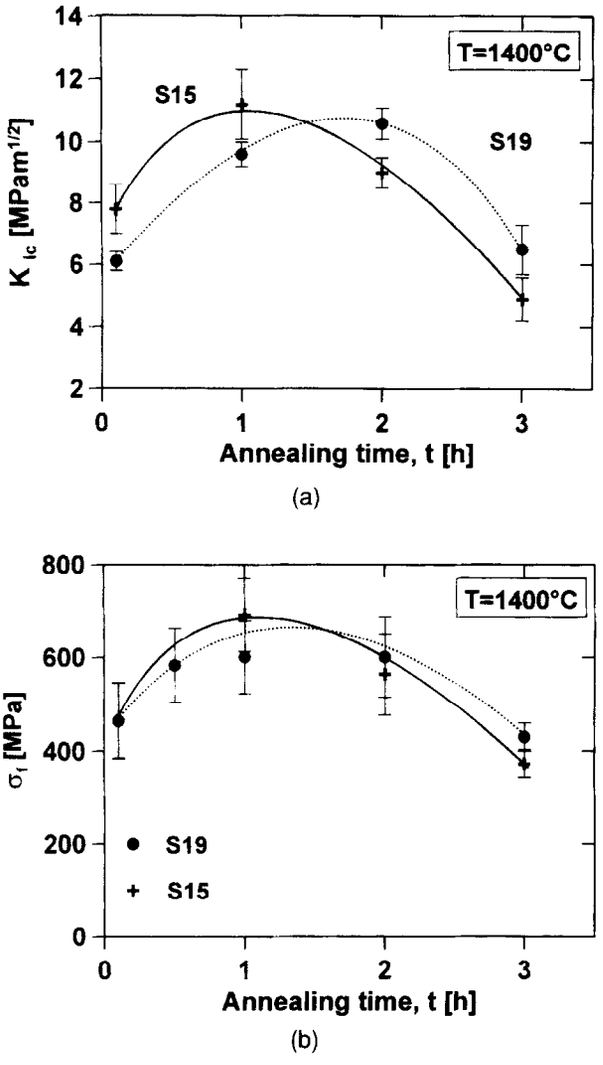

Fig. 8. (a) Fracture toughness and (b) fracture strength of eutectoidly aged S15 and S19, respectively.

3.2 Hot isostatically pressed (Mg,Y)-PSZ

3.2.1 Microstructure

Hot isostatically pressed samples appear dark brown instead of white due to an understoichiometric composition. The general microstructure resembles that of sintered specimens with a mean grain size of 18 μm. However, the small homogeneously distributed pores are eliminated (Fig. 9). In the as-sintered state, no transformable t-phase was detected. In analogy to the pressureless sintered material, the amount of transformable t-phase can be enhanced by eutectoid ageing at 1400°C. As shown in Fig. 3, an amount of up to 31 vol% can be achieved after 1 h of ageing in nitrogen. The amount of m-phase increases simultaneously from 0 to 14 vol%.

3.2.2 Failure origins

Fracture surfaces from broken bend bars are shown in Fig. 10. Again, the fracture mode is purely transgranular. However, the size of failure origins is reduced remarkably as compared to the sintered material. Obviously, also the large pores are eliminated. As failure origins, agglomerates of spinel with a size smaller than 15 μm were identified.

Fig. 9. Microstructure of HIPed (Mg,Y)-PSZ with 3 vol% $MgAl_2O_4$ spinel. Spinel particles appear within the pore-free bulk as black.

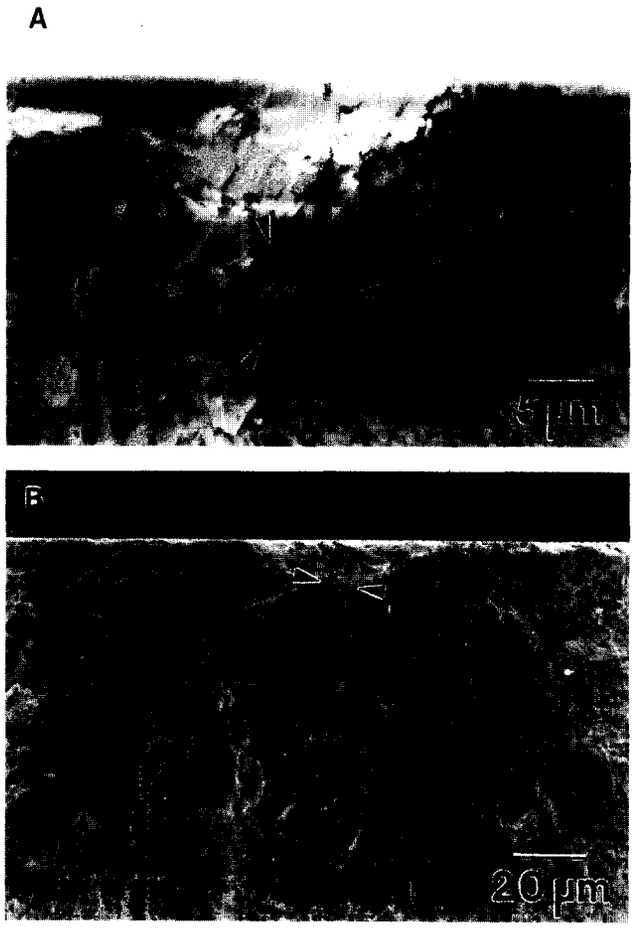

Fig. 10. Fracture surface of unaged HIP19 in (a) failure origin and (b) fracture mirror.

3.2.3 Stress-strain behaviour

The stress-strain curves for aged and unaged specimens are shown in Fig. 11. While unaged specimens do not show any plastic deformation,

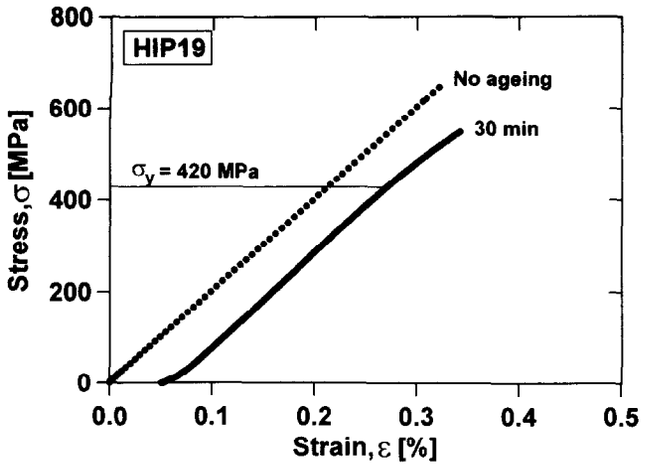

Fig. 11. Stress-strain curves of unaged and aged HIP19.

the aged high-toughness material shows onset of t → m transformation at a yield stress of 420 MPa. Again plastic deformation could be discerned on the tensile side of bend bars after fracture (Fig. 7(b)). The critical stresses for transformation calculated from the yield stresses are compared to the equivalent values for sintered materials in Table 1.

3.2.4 Mechanical properties

Fracture toughness is improved by ageing treatment from 4·9 ± 0·4 in the as-HIPed material to 10·2 ± 0·8 MPa √m after 1 h ageing (Fig. 12). Peak strength in the HIPed material does not correlate with peak toughness. The highest strength of 878 ± 56 MPa is achieved after 30 min ageing at a fracture toughness of 7·0 MPa √m. At the highest toughness (10·2 MPa √m), the strength is reduced to 768 ± 29 MPa.

4 Discussion

4.1 Microstructure

Fine-grained (Mg,Y)-PSZs with grain sizes between 13 and 19 μm are achieved with pressureless sintering as well as with HIPing. The key to obtain this structure is the spinel additions which act as grain growth inhibitor.

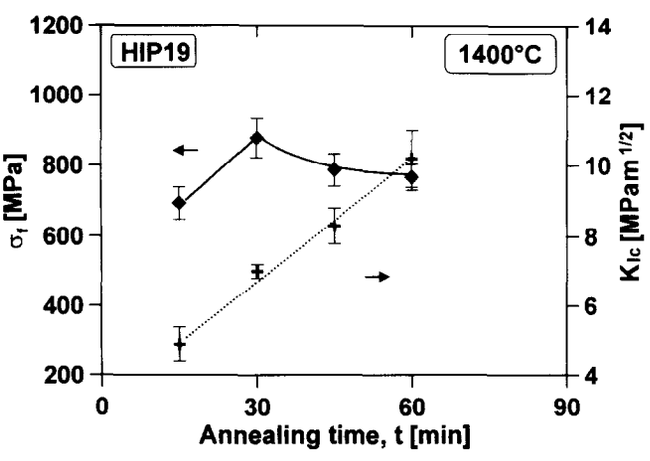

Fig. 12. Fracture strength and toughness of HIPed (Mg,Y)-PSZ as a function of ageing time.

The amount of transformable t-phase after sintering is determined by the cooling rate which governs the size of t-precipitates. While cooling rates of either 15 or 19 K/min lead to small sizes able to allow good control of the amount of transformable t-precipitates by subsequent eutectoid ageing, lower cooling rates lead to premature ripening and formation of metastable t-precipitates during cooling. Using 6 K/min the as-sintered material is nearly peak-aged as indicated by a K_{Ic} of 9·5 MPa √m and an amount of 30 vol% of transformable t-phase. Lower cooling rates as 6 K/min or subsequent ageing would overage the t-precipitates and would cause severe degradation.

The amount of about 30 vol% t-precipitates which can be obtained in rapidly cooled pressureless sintered (Mg,Y)-PSZ by eutectoid ageing for 1–2 h is comparable to that of conventional Mg-PSZ. Hence, the precipitation behaviour of the t-phase is nearly identical to that of Mg-PSZ.[6] It is noteworthy that, also in hot isostatically pressed (Mg,Y)-PSZ, an amount of 30 vol% transformable t-phase can be achieved by eutectoid ageing. Earlier attempts to hot press or hot isostatically press Mg-PSZ to produce transformable t-precipitates by ageing in air have failed.[18,19] A prerequisite is that ageing is performed in nitrogen. Preliminary experiments have shown that also in (Mg,Y)-PSZ an ageing treatment in air at 1100°C for 30 min leads to spontaneous transformation. It is believed that oxygen deficiency due to nitrogen incorporation is involved as stabilising mechanism as has been stated earlier for unstabilised zirconia and Y-TZP.[25,26] The subsequent ageing in air causes a release of nitrogen and a loss of related additional oxygen vacancies. As a consequence, spontaneous transformation occurs.

Peak ageing occurs for both sintered and HIPed materials at nearly the same ageing time. This result is somewhat surprising because the higher oxygen vacancy concentration should lead to a larger critical size of the t-precipitates. Consequently, peak ageing should occur at longer ageing times. An explanation may be that the t-precipitates in HIPed samples grow faster due to a higher local temperature in the hot isostatic press. As a consequence, t-precipitates in HIPed samples are as metastable as those in sintered samples after the same ageing time.

4.2 Failure origins

As evident from the fracture surfaces, the failure origins are large pores in all pressureless sintered samples regardless of ageing time. Although the

critical stress for transformation in high-toughness samples is well below the fracture stress, plastic deformation and microcracking has been observed on tensile sides. It is concluded from such observation that maximum strength occurs at maximum toughness that even in high-toughness samples strength is flaw-size-controlled. This is in contrast to other high-toughness zirconias like Mg-PSZ and Ce-TZP where strength is transformation-controlled and strength decreases with increasing toughness.[7]

The origin of the large pores cannot yet be clarified. Preliminary experiments point to their formation at temperatures > 1500°C. Evaporation of MgO as well as burning out of strongly bonded organic substances must be taken in consideration.

Presintering at 1500°C and subsequent hot isostatic pressing eliminates the large pores. Because hot isostatic pressing is known to eliminate small pores in ceramic materials very effectively, but not pores larger >100 μm[27,28] it is not likely that the pores with diameters up to 160 μm were simply compressed by HIPing. We suggest therefore that the pressure applied below 1500°C readily suppresses pore formation. By inspecting the fracture surfaces, this appears as a reduction in flaw size in the low-toughness specimens. The observation that the strength in HIPed specimens is reduced with increasing toughness leads to the conclusion that strength in this regime is transformation-controlled. Apparently, the generated surface cracks can compete in this case with the inherent defects.

4.3 Mechanical properties

The high amount of transformable t-phase after eutectoid ageing, due to transformation toughening, allows for an increase in fracture toughness up to ~11 MPa $\sqrt{m}$ in both pressureless sintered and HIPed (Mg,Y)-PSZ. Hence, by exploiting transformation toughening, the strength of unaged specimens of both pressureless sintered and HIPed (Mg,Y)-PSZs can be remarkably improved.

The strength of pressureless sintered samples is determined by the size of the large pores which, in the pressureless sintered materials, are much larger than the grain size. The difference in grain size has therefore only a negligible influence on strength. Therefore, the fine-grained microstructure could not be exploited for strength improvement. The defect size is comparable to that of Mg-PSZ and consequently, a strength higher than 700 MPa cannot be expected. Indeed, the maximum strength of 600–700 MPa coincides with that of peak-strength Mg-PSZs where strength is limited by grain boundary fracture.[29]

The experiments using hot isostatic pressing have shown that the fine-grained microstructure can be utilised, as the large pores occurring in sintered (Mg,Y)-PSZs are eliminated. Due to the reduction in flaw size, the strength of the unaged hot isostatically pressed material is considerably enhanced. With respect to the unaged S19 material the strength is doubled and is already in the order of peak-strength Mg-PSZ or peak aged sintered (Mg,Y)-PSZ. Because stable crack growth cannot be expected in unaged HIPed and pressureless sintered materials due to small R-curve behaviour, the equivalent defect size has to be approximately four times smaller in the latter. Comparing the mean defect sizes of 60 and 15 μm, this ratio of 4 is verified and hence the increase in strength in the HIPed material is accounted for.

When fracture toughness is additionally enhanced by transformation toughening, the small flaw size allows for further strength improvement in HIPed samples to about 900 MPa. At fracture toughness values higher than 7 MPa $\sqrt{m}$, the strength is limited by transformation-induced yielding. The critical stress for transformation is then considerably below the fracture stress and plastic deformation and microcracking attributed to the phase transformation occurs. While the inherent flaw size is large in pressureless sintered samples and a very low critical stress is required in order to produce a surface crack of comparable size, yielding becomes important only at high K_{Ic} values in these materials. In HIPed samples, small surface flaws generated at high critical stresses are sufficient to compete with inherent flaws. When larger than 15 μm their growth along the specific R-curve causes final failure. As a result, strength is transformation-limited. The interrelation between flaw size, transformability, R-curve behaviour and strength of fine-grained (Mg,Y)-PSZ is outlined in a forthcoming paper.[30]

5 Conclusions

1. Fracture strength and fracture toughness in fine-grained (Mg,Y)-PSZ can be favourably adjusted by either changing cooling rate or eutectoid annealing time.
2. Strength in sintered (Mg,Y)-PSZ is controlled by pores up to 100 μm.
3. Fracture strength and fracture toughness of sintered (Mg,Y)-PSZ are comparable to those of Mg-PSZ.
4. HIPing yields reduced defect size and increased strength in as-fired specimen up to 700 MPa at toughness of 4·9 MPa $\sqrt{m}$.
5. With eutectoid ageing, strength and toughness of HIPed samples can be improved considerably. Peak strengths of about 900 MPa

are obtained at a toughness of 7 MPa $\sqrt{m}$. Longer annealing further increases toughness but reduces strength. The origin is a change from defect- to transformation-controlled failure.

Acknowledgement

The authors thank M. V. Swain for helpful discussions.

References

1. Heuer, A. H., Readey, M. J. & Steinbrech, R., Resistance curve behavior of supertough MgO-partially-stabilized ZrO_2. *Mater. Sci. Eng.*, **A105/106** (1988) 83–89.
2. Dauskhardt, R. H., Marshall, D. B. & Ritchie, R. O., Cyclic fatigue-crack propagation in magnesia-partially-stabilized zirconia ceramics. *J. Am. Ceram. Soc.*, **73**(4) (1990) 893–903.
3. Hoffmann, M. J., Dauskhardt, R. H., Ager, J., Mai, Y.-W. & Ritchie R. O., Grain size effects on cyclic fatigue and crack-growth resistance behaviour of partially stabilized zirconia. *J. Mater. Sci.*, **30** (1995) 3291–3299.
4. Hannink, R. H. J. & Swain, M. V., Magnesia-partially stabilized zirconia: The influence of heat treatment on thermomechanical properties. *J. Austr. Ceram. Soc.*, **18**(2) (1983) 53–62.
5. Green, D. J., Hannink, R. H .J. & Swain, M. V., *Transformation Toughening of Ceramics*. CRC Press, Boca Raton, FL, 1989.
6. Hannink, R. H. J., Howard, Ch.J., Kisi, E. H. & Swain, M. V., Relationship between fracture toughness and phase assemblage in Mg-PSZ. *J. Am. Ceram. Soc.*, **77**(2) (1994) 571–579.
7. Swain, M. V. & Rose, L. R. F., Strength limitations of transformation-toughened zirconia alloys. *J. Am. Ceram. Soc.*, **69**(7) (1986) 511–518.
8. Marshall, D. B., Strength characteristics of transformation-toughened zirconia. *J. Am. Ceram. Soc.*, **69**(3) (1986) 173–180.
9. Swain, M. V., Limitation of maximum strength of zirconia-toughened ceramics by transformation toughening increment. *J. Am. Ceram. Soc.*, **68**(4) (1985) C-97–C-99.
10. Heuer, A. H., Transformation toughening in ZrO_2-containing ceramics. *J. Am. Ceram. Soc.*, **70**(10) (1987) 689–698.
11. Claussen, N., Microstructural design of zirconia-toughened ceramics (ZTC). In *Advances in Ceramics*, Vol. 12, *Science and Technology of Zirconia II*, ed. N. Claussen, M. Rühle & A. H. Heuer. The American Ceramic Society, Columbus, OH, 1984, pp. 325–351.
12. Meschke, F., De Portu, G. & Claussen, N., Microstructure and thermal stability of fine-grained (Y,Mg)-PSZ ceramics with alumina additions. *J. Eur. Ceram. Soc.*, **11** (1993) 3951–3956.
13. Meschke, F., De Portu, G. & Claussen N., Preparation and characterization of fine-grained (Mg,Y)-PSZ ceramics with spinel additions. In *Science and Technology of Zirconia V*, ed. S. Badwal, J. Bannister & R. Hannink. Technomic Publishing, Lancaster, PA, 1993, pp. 99–107.
14. Meschke, F., De Portu, G., Claussen, N. & Rödel, J., Phase stability of fine-grained (Mg,Y)-PSZ. *J. Am. Ceram. Soc.*, **78**(7) (1995) 1997–1999.
15. Farmer, S. C., Heuer, A. H. & Hannink, R. H. J., Eutectoid decomposition of MgO-partially stabilized ZrO_2. *J. Am. Ceram. Soc.*, **70**(8) (1987) 431.
16. Hannink, R. H. J., Microstructural development of sub-eutectoid aged MgO–ZrO_2 alloys. *J. Mater. Sci.*, **18** (1983) 457.
17. Scott, H. G., Phase relations in the magnesia-yttria-zirconia system. *J. Austr. Cer. Soc.*, **17**(1) (1981) 16–20.
18. Dworak, U., Olapinski, H. & Burger, W., Thermal stability in PSZ. In *Advances in Ceramics* Vol. 24A: *Science and Technology of Zirconia III*, ed. S. Somiya, N. Yamamoto & H. Yanagada. The American Ceramic Society, Columbus, OH, 1988, pp. 545–548.
19. Hogg, C. L., Stringer, R. K. & Swain, M. V., Grain-boundary cavitation and bloating of isostatically hot-pressed magnesia-partially-stabilized zirconia on air annealing. *J. Am. Ceram. Soc.*, **69**(3) (1986) 248–251.
20. Stevens, R. & Yuksel, A., Grain-grain boundary precipitation phenomena and related mechanical properties in dense (hot pressed) Mg-PSZ. *Br. Ceram. Trans.*, **83** (1984) 146–150.
21. Nishida, T., Shiono, T., Nagai, A. & Nishikawa, T., Evaluation of fracture toughness for structural ceramics using SEPB specimens. *J. Ceram. Jpn Inter. Edn*, **96** (1988) 597–602.
22. Nose, T. & Fujii, T., Evaluation of fracture toughness for ceramic materials by a single-edge-precracked-beam method. *J. Am. Ceram. Soc.*, **71**(5) (1988) 328–333.
23. DIN51109, *Testing of High Performance Ceramics, Fracture Toughness* (in German). Beuth Verlag, Berlin (1991).
24. DIN51110, Part 1, *Testing of High Performance Ceramics, 4-point Bending at Room Temperature* (in German). Beuth Verlag, Berlin (1990).
25. Claussen, N., Wagner, R., Gauckler, L. J. & Petzow, G., Nitride-stabilized cubic zirconia. *J. Am. Ceram. Soc.*, **61**(7-8) (1978) 369–370.
26. Cheng, Y.-B. & Thompson, D. P., Role of anion vacancies in nitrogen-stabilized zirconia. *J. Am. Ceram. Soc.*, **76**(3) (1993) 683–688.
27. Kellett, B. J. & Lange, F. F., Experiments on pore closure during hot isostatic pressing and forging. *J. Am. Ceram. Soc.*, **71**(1) (1988) 7–12.
28. Uematsu, K., Sekiguchi, M., Kim, J. Y., Saito, K., Mutoh, Y., Inoue, M., Fujino, Y. & Miyamoto, A., Effect of processing conditions on the characteristics of pores in hot isostatically pressed alumina. *J. Mater. Sci.*, **28** (1993) 1788–1792.
29. Govila, R. K., Strength characterization of MgO-partially stabilized zirconia, *J. Mater. Sci.*, **26** (1991) 1545–1555.
30. Meschke, F., Claussen, N. & Rödel, J., Interrelation between transformability, *R*-curve behavior and fracture strength in fine-grained (Mg,Y)-PSZ *J. Am. Ceram. Soc.*, in press.